Human-driven temporal shifts in fire activity: southwest Russia and north Australia as case study regions

Tianjia Liu[1], Loretta J. Mickley[2], and Jessica L. McCarty[3]

[1]Department of Earth and Planetary Sciences, Harvard University, Cambridge, MA, USA
[2]John A. Paulson School of Engineering and Applied Sciences, Harvard University, Cambridge, MA, USA
[3]Department of Geography, Miami University, Oxford, OH, USA

Abstract

Decadal trends in fire activity can reveal important human and climate-driven influences across a multitude of landscapes from croplands to savannas. We use 16 years of daily satellite observations from 2003-2018 to search globally for stationary temporal shifts in fire activity during the primary burning season. We focus on southwest Russia and north Australia as case study regions; both regions experienced nearly 40-day shifts over a 16-year period but in opposite directions. In southwest Russia, a major wheat-growing region, we trace the delay in post-harvest fires to several potential drivers: modernization in the agricultural system and recent droughts, followed by government restrictions on wheat exports. In north Australia, prescribed burns in the early dry season are a key practice in Aboriginal fire management of savannas, and the increasing trend of such fires has limited the size and extent of fast-spreading late dry season fires, thereby shifting overall fire activity earlier. In both regions, human action, through controlling fire ignition and extent, is likely the dominant driver of the temporal shifts in fire activity with climate as both a harbinger and an amplifier of human-induced changes.

1. Introduction

Two decades of daily satellite data from NASA's Moderate Resolution Imaging Spectroradiometer (MODIS) have made analysis of long-term trends in global fire activity possible at daily scale (Andela *et al* 2017). While climate variability is a dominant control on fire activity, humans play an important role in modulating fire behavior through ignition, fire suppression and management, and land use change (Andela and van der Werf 2014, Andela *et al* 2017, Chen *et al* 2017, Pechony and Shindell 2010, Riley *et al* 2019, Bowman *et al* 2020). Andela et al. (2017) mainly attribute the 24% decline in global burned area from 1998-2015 to human activity, through expansion in populated areas, croplands, and livestock, rather than variability in precipitation or temperature. Understanding trends in fire activity can (1) shed light on the consequences of changes in local land management practices and agricultural systems and (2) lead to efforts to mitigate fire-related impacts on air quality, public health, ecosystem services, and the carbon budget (Koplitz *et al* 2016, Johnston *et al* 2012, Liu *et al* 2016, Zhang *et al* 2014a, Bowman *et al* 2020).

While most studies to date have investigated global trends in the magnitude of fire activity (e.g., Andela et al., 2017), here we focus on regional shifts in the timing of peak fire activity. Regions with large, sustained temporal shifts over a multi-year period may reveal

human influence on fire regimes through management or land use. In forest management, controlled burning of fuel-abundant areas in advance of the fire season peak can reduce the number and size of large fires (Fernandes and Botelho 2003). An earlier fire season suggests better managed forests with fewer large and destructive fires, while a later fire season would indicate the opposite. In croplands, recent work using satellite fire data identified a primarily human-driven delay in rice residue burning in north India (Liu *et al* 2020a, Jethva *et al* 2019, Balwinder-Singh *et al* 2019). In this region, the ~2-week shift in the post-monsoon fire season from late October to early November from 2003-2018 can be partially attributed to a 2009 groundwater policy that delayed rice planting dates closer to the summer monsoon onset. The policy, which arose from an effort to combat the severe groundwater decline (Singh 2009, Tripathi *et al* 2016), unleashed a cascade of effects that delayed the rice growing season and subsequent burning of rice residues, with unintentional consequences for air quality (Liu *et al* 2020a, Jethva *et al* 2019, Balwinder-Singh *et al* 2019). This is because burning later in the year coincides with meteorological conditions that favor the accumulation of pollutants — i.e., weak ventilation from temperature inversions, stagnant winds, and low mixing layer heights (Ojha *et al* 2020).

To fully understand the potential of temporal shifts in the fire season to signal human imprints and influence regional air quality and human health, we must first identify such regions. In this study, we search globally and uncover additional regions with notable temporal shifts in fire activity from 2003-2018. We further investigate two case study regions, southwest Russia and north Australia, where we observe particularly large temporal shifts of nearly 40 days during the primary fire season in opposite directions — later in Russia and earlier in Australia. Finally, we probe and discuss possible human and climatic influences on temporal shifts in the two case study regions, and briefly, on a global scale.

2. Data and Methods

2.1 Satellite fire datasets

As two measures of fire activity, we use the Level 3 MODIS Collection 6 burned area (MCD64A1) and active fire (MOD14A1/MYD14A1) products (Table S1). MCD64A1 is available in monthly timesteps from 2000-present at 500-m spatial resolution (Giglio *et al* 2018). We disaggregate MCD64A1 burned area to daily timesteps according to the Julian burn date. The MOD14A1 and MYD14A1 gridded active fire products are available daily at 1-km spatial resolution for the Terra (10:30 am/pm) and Aqua (1:30 am/pm) satellite overpasses, respectively (Giglio *et al* 2016). For each day, we combine MOD14A1 and MYD14A1 active fires (hereafter referred to as MxD14A1) into a binary fire mask (0 = no fire, 1 = fire), a custom product for this analysis that is different than the MCD14ML global monthly fire location product (Giglio *et al* 2016). To reduce noise at the pixel level, we sum daily MCD64A1 burned area and MxD14A1 active fire area on a 0.25° x 0.25° grid. More details about the satellite fire datasets are provided in Supplementary Section S1.

2.2 Global search for temporal shifts in the primary fire season

As an initial search for temporal shifts, we focus on a 16-year time period from 2003-

2018 but include observations in 2002 if the primary fire season for a particular grid cell extends from December to January of the following year. In brief, our approach, following Liu *et al* (2020a, 2020b), is to track the changes in the midpoint of the primary fire season, $k_{midpoint}$, defined as the mean of days k, weighted by daily burned area (BA_k):

$$k_{midpoint} = \frac{\sum_{k=1}^{n} (k \times BA_k)}{\sum_{k=1}^{n} BA_k} \qquad (1)$$

For each grid cell, we define the primary fire season as a 7-month time window centered on the month with the highest burned area but exclude those months with < 1% annual burned area; we use $k = 1, 2, 3 \ldots n$ to represent days of the fire season. For each grid cell, we take the slope of a simple linear regression of the yearly $k_{midpoint}$ timeseries as the magnitude of the temporal shift in the fire season, in days per year. In this initial step, we define a lax threshold of $p < 0.1$ as statistically significant to more easily identify clusters of grid cells with temporal shifts and define regions of interest (ROIs). We further exclude grid cells with < 5 years of BA observations to focus on stationary temporal shifts.

Because of this focus on areas where fires recur on an annual basis at similar intensity, potential ROIs consist primarily of cropland and savanna, grassland, and shrubland areas rather than forested areas. We use the MODIS MCD12Q1 land cover product with the University of Maryland (UMD) classification to assign the primary land cover for each ROI (Sulla-Menashe *et al* 2019). We further investigate two ROIs as our case studies: southwest Russia and north Australia (Figure 1, Table 1), where the temporal shifts in the primary fire season are particularly large (> 1 month from 2003-2018) and spatially cohesive. For each ROI, we refine the start and end dates of the primary fire season based on the time series of daily regional BA stacked by Julian day from 2003-2018. As described above, our initial global search to identify ROIs uses a generalized 7-month window centered on the month with the highest burned area.

Additionally, the very different geographical context of these two ROIs — croplands in southwest Russia and savannas in north Australia — allows us to juxtapose the potential land cover and region-specific mechanisms that led to the temporal shifts. Fires in both regions are heavily impacted by human activity, either through agricultural practices or fire management. For case study 1, we define southwest Russia as Krasnodar Krai, Republic of Adygea, Rostov Oblast, and Stavropol Krai, which are major wheat-growing areas located in the North Caucasus and Southern Federal Districts to the east of the Black Sea (Figure S2a). This region, with its fertile black soils and favorable climate, produces over half of Russia's winter wheat, with ~25% higher yields than the all-Russia average (ROSSTAT 2020b, Schierhorn *et al* 2014; Figure S3). For case study 2, we define north Australia as areas north of 14.75°S in the Top End of Northern Territory and Cape York in Queensland. We focus on Arnhem Land, a biodiverse region in the eastern half of the Top End, has a majority Aboriginal population, large Indigenous protected lands, and a network of Indigenous ranger groups (Price *et al* 2012, Russell-Smith *et al* 2019, Ansell *et al* 2020; Figure S5a).

For our two case study regions, southwest Russia and north Australia, we use two methods to estimate $k_{midpoint}$: 1) weighted mean (as described in Section 2.1) and 2) sigmoid-smoothed partial sums (Zhang *et al* 2014b). Both methods have been used to characterize the temporal progression of the fire season (Zhang *et al* 2014b, Liu *et al* 2020a); moreover, the two

methods show minimal differences in the derived temporal shifts in the fire season (Liu *et al* 2020b). In method 2, $k_{midpoint}$ is defined as the first day by which 50% of total fire activity as indicated by area burned has occurred. To reduce the sensitivity of this method to large spikes in fires, we apply sigmoid smoothing to the partial sums before calculating $k_{midpoint}$. Hereafter, we abbreviate $k_{midpoint}$ from method 1 as $k_{midpoint}, \omega$ and that from method 2 as $k_{midpoint}, \rho$. We find that applying sigmoid smoothing in method 2 increases agreement between $k_{midpoint}, \omega$ and $k_{midpoint}, \rho$. While method 1 is computationally efficient for our initial global search, method 2 allows us to more accurately characterize the start and end of the fire season, k_{start} and k_{end}, for fire seasons with asymmetrical temporal distributions. We define k_{start} and k_{end} as the day by which 10% and 90%, respectively, of total burned area for that season has accumulated. Here for our case study regions, we define $p < 0.05$ as statistically significant.

Ancillary datasets and methods used to provide context on the potential links between fires, human activity, and meteorology are described in Supplementary Section S2.

3. Results and Discussion

3.1 Global temporal shifts in fire activity

We detect temporal shifts in 22% of global burned area using MCD64A1 and 25% using MxD14A1 active fire area at a statistical significance threshold of $p < 0.1$ (Figure 1). However, we note that some grid cells with temporal shifts are spatially fragmented or opposite in sign relative to their neighbors. This "speckle" may be characteristic of a mismatched grid cell size for analysis where it is incompatible with the process being observed (i.e. non-stationary) or statistical noise. Instead, we focus on large clusters of grid cells with similar magnitudes and the same sign in temporal shifts, so that when burned area is aggregated over the defined ROI, the overall temporal shift is likely statistically significant as well. In Figure 1, we highlight select ROIs with coherent temporal shifts for croplands (northwest India, southwest Russia, south Russia, and Thailand) and for savannas, grasslands, and shrublands (north Australia, central Madagascar, Zimbabwe, and north Brazil). However, other clusters may be present, such as within the African Sahel, where the spatial patterns of temporal shifts are complex.

In the following sections, we delve into the two case study regions, southwest Russia (Section 3.2) and north Australia (Section 3.3), which see large temporal shifts of 2.41 days yr^{-1}, or a total of 39 days from 2003-2018 (Table 1, Figure 2). In the other ROIs, not discussed in detail here, we observe temporal shifts of 1.36 days yr^{-1} (22 days earlier) in south Siberia, Russia, 0.64 days yr^{-1} (10 days later) in Thailand, 1.99 days yr^{-1} (32 days earlier) in central Madagascar highlands, 0.81 days yr^{-1} (13 days later) in Zimbabwe, and 0.61 days yr^{-1} (10 days later) in the state of Pará, Brazil (Table 1, Figure S1). We conclude with a discussion of the drivers of temporal shifts in fire activity (Section 3.4).

3.2 Case study 1: southwest Russia

The primary fire season in southwest Russia croplands extends from summer to autumn, mainly from late June to October, after the winter wheat harvests (Hall *et al* 2016, Korontzi *et al* 2006; Figure 3a-b). We estimate that the midpoint of the fire season has shifted later by 2.41

days yr^{-1}, or 39 days from 2003 to 2018 (Table 1, Figure 2a, Figure S2). This shift is consistent across breakpoints in the fire season, varying from 2.3 to 2.82 days yr^{-1}, and driven largely by a 95% decrease in fires from June to July and a 41% increase in September.

Here the example of northwest India described above can inform our case study on southwest Russia, as both involve water-stressed agricultural systems. In northwest India, state government policies delayed rice sowing to alleviate heavy groundwater usage prior to the monsoon onset; in turn, post-monsoon rice harvests and subsequent burning of rice residues shifted later. For southwest Russia, we discuss two potential drivers of the delay in fire activity: (1) improved management, investment, and productivity in the agricultural sector and (2) groundwater depletion and drought, followed by federal government policies, such as wheat export restrictions and bans.

First, since the early 2000s, the region has experienced the rise of "agroholdings," a new type of agricultural enterprise that acquires corporate farms and efficiently manages end-to-end production, processing, and distribution (Rada *et al* 2017). Rada *et al* (2017) attributes the high productivity in southwest Russia to these agroholdings, as well as to the favorable climate and soils and proximity to Black Sea ports. Puzzlingly, the 132% increase in winter wheat production in the region, and by extension the volume of crop residues, coincides with a 77% decrease in burned area since 2005 (Figure S3). This is opposite of the trend in northwest India, where the rise in rice production and adoption of mechanization (i.e., use of combine harvesters) led to an increase in rice residue burning (Liu *et al* 2019, Shyamsundar *et al* 2019). This discrepancy between the regions may exist for two reasons. First, wheat residue is more suitable for livestock feed than rice residue, which has high silica content, so there may be greater utility for residue in southwest Russia than in north India (Sidhu *et al* 2015). Second, modernized agriculture systems in southwest Russia may have driven changes in crop residue management, wherein farmers use fire less to remove wheat residues immediately post-harvest (around July) and more to clear residual waste on fields just prior to sowing (around September) (Figures 2a, 3a-b). In contrast, the short turnaround period (on the order of weeks) between crops in the rice-wheat rotation of northwest India (Vadrevu *et al* 2011), means that Indian farmers depend on fire to rapidly clear their fields (Figure 3a; Liu *et al* 2020). Consistent with this hypothesis, the average fire intensity per active fire detection peaks in July and decreases by 41% by September (Figure S4).

In addition, Rostov farmers surveyed by the U.S. Department of Agriculture (USDA) claim that only small enterprises still burn to reduce risk of soil-based diseases affecting crop growth (Hall *et al* 2016). Greater alternative uses for wheat residue, as mentioned above, and the availability of direct seeding or no-till technology may explain the declining use of fire as a primary tool for crop residue management. For example, Krasnodar farmers typically embed loose wheat residues into soil as a fertilizer and to prevent soil degradation (Sidorenko *et al* 2017). Additionally, wheat residues may be baled for livestock feed, in view of the resurgence in the livestock sector in the 2000s due to government policies and investment (Liefert and Liefert 2012, Fellmann *et al* 2014, Rada *et al* 2017). As early as 2014, civil society organizations invested in agricultural outreach and training to eliminate agricultural burning in Krasnodar and Rostov (ICCI 2020). Evidence of a link between the temporal shift in the fire season in southwest Russia and modernization in the agricultural system may be found in the record of wheat yields, which are correlated to fertilizer use and farm machinery efficiency (Liefert *et al*

2013, Deppermann *et al* 2018). Indeed, we see higher winter wheat yields and temporal shifts in Krasnodar and Adygea (+2.69-2.8 days yr^{-1}, $p < 0.05$) than in Rostov and Stavropol (+1.59-1.93 days yr^{-1}, $p < 0.05$) (Figure S3, Table S4).

Second, high water withdrawal for competing uses in residential, industrial, and agricultural sectors has led to moderate to severe water stress in southwest Russia (Alcamo *et al* 2007). Rodell *et al* (2018) attributes the downward trend in freshwater storage from 2003-2016 to groundwater depletion and drought. Within our study region, GRACE observations indicate a decrease in freshwater availability of 1.43 cm yr^{-1} (Figure 3d), which is comparable to that in northwest India (-1.44 cm yr^{-1}). In particular, changes in vapor pressure deficit (VPD) are most pronounced during summer and early autumn days, with increases up to ~30-70 Pa yr^{-1} from 2003-2018 (Figure 3c). Dryness can delay winter wheat sowing (Wegren 2011, USDA 2020), which may partly explain the increase in late season fires. Additionally, drought in tandem with federal government policies may have exacerbated delays in winter wheat sowing in this region. In August 2010, after intense heatwaves, drought, and wildfires devastated crop production elsewhere in Russia, the government banned wheat exports in an effort to stabilize domestic food prices (Wegren 2011; Figure 3e). While southwest Russia was spared damage to its winter wheat, the export ban disrupted the supply chain in this region, and wheat prices plummeted (Wegren 2011, ROSSTAT 2020a). Anecdotally, some farmers in Krasnodar waited to sell their wheat crop to return a higher profit (de Sousa 2019), and the wheat price then strongly rebounded. In contrast, no export restrictions were imposed in 2012, a severe drought year with low wheat production and exports similar to those in 2010 (Götz *et al* 2016). Nevertheless, like in 2010, wheat producer prices in 2012 sharply rose starting in July, indicating that farmers may have again waited to sell their wheat crop (Figure 3e). These price swings and related delays in selling wheat may have also delayed sowing if farmers relied on these profits to buy seeds and fertilizer for the following year's crop.

In summary, factors that may have driven the 39-day delay in fires in southwest Russia include improvements in agricultural management and technology, drought and groundwater depletion, and fluctuations in wheat prices due to export restrictions and bans.

3.3 Case study 2: north Australia

The primary fire season in the savannas of north Australia occurs during the dry season primarily from May through November. We estimate that the midpoint of the fire season has shifted by -2.41 days yr^{-1}, or 39 days earlier from 2003-2018 (Table 1, Figure 2b, Figure S6). This shift is consistent across breakpoints in the fire season, varying from -3.06 to -2.29 days yr^{-1}. We find the trend is induced by a 40% increase during the early dry season (EDS) from May to July and a 67% decrease in fires during the late dry season (LDS) from September to November, with the transition point from the EDS to LDS defined as July 31 (Price *et al* 2012).

During the LDS, fires tend to burn out of control due to favorable fire weather, such as high VPD values. The resurgence of Aboriginal fire management practices in north Australia, which began in the 1990s, has spurred the decrease in fires during the LDS, most notably in Arnhem Land (Yibarbuk *et al* 2001, Whitehead *et al* 2003, Price *et al* 2012, Price 2015, Ansell *et al* 2020, Evans and Russell-Smith 2020; Figure S9a). Since 2005-06, the West Arnhem Land Fire Abatement (WALFA) project has built on the collaboration with Indigenous fire managers

and landowners to reduce greenhouse gas emissions by curbing large, destructive fires in the LDS (Price *et al* 2012, Ansell *et al* 2020). Following WALFA, there are four other ALFA projects in operation: CALFA (central Arnhem), NEALFA (northeast Arnhem), SEALFA (southeast Arnhem), and SEALFA Stage 2 (Price 2015, Ansell *et al* 2020). In the past decade, dozens of savanna burning projects in the Top End have emulated WALFA. Registered under the Australian government's Carbon Credits (Carbon Farming Initiative) Act 2011 and Emissions Reduction Fund, these projects can earn Australian carbon credit units (ACCUs) (Ansell *et al* 2020; Figure S6). The economic incentive for Aboriginal people involved in these carbon abatement projects adds to inherent environmental, social, and cultural co-benefits of such projects (Andersen *et al* 2005, Ansell *et al* 2020).

Our results provide quantitative evidence of the success of these policy efforts to reduce fire size, especially later in the dry season when fires are more likely to burn out of control. We find that fire management within the savanna burning project areas in the Top End and Cape York drives the temporal shifts toward an earlier fire season, with spatially cohesive shifts within the domain of Aboriginal freehold lands and ALFA projects. This domain accrued over 2.5 million ACCUs from 2012-13 to 2018-19 (Figures S5-6). Within the study region, we find a temporal shift in the midpoint of the primary fire season of -3.48 days yr^{-1} ($p < 0.05$) in savanna burning project areas, which comprise ~56% of the annual burned area, compared to just -0.9 days yr^{-1} in other areas ($p = 0.18$) (Table S5). Moreover, ALFA project areas, which have a long history of fire management (Price *et al* 2012, Price 2015, Ansell *et al* 2020), exhibit a higher overall temporal shift of -4.3 days yr^{-1} ($p < 0.05$), particularly in WALFA at -6.13 days yr^{-1} ($p < 0.05$), than the region overall.

In north Australia fire management, prescribed burning creates a mosaic of burned and unburned areas during the EDS, decreasing overall fuel availability across the landscape (Andersen *et al* 2005, Trauernicht *et al* 2015, Russell-Smith *et al* 2019). The fuel-limited areas, where prescribed burning has occurred, act like a patchwork of endpoints for fast-spreading wildfires in the LDS, thus limiting the maximum extent of the final burn perimeters (Price *et al* 2012, Petty and Bowman 2007, Petty *et al* 2015). This phenomenon is widespread across Arnhem Land, where small fires have become more prevalent during the EDS and widely dispersed across the landscape (Figure 3a-d). During the EDS, we see a 60% decline in the average distance to the closest fire and a 50-60% increase in the number of distinct fire perimeters from 2003-2018 (Figure 4e). The increase in EDS fires and their spatial coverage suggest fewer open spaces for fires later in the season to spread across, and indeed, we see a 49-54% decrease in the average area per fire during the LDS (Figure 4f). The decrease in LDS fire activity is consistent across burned area and fire emissions datasets, as described in Supplementary Section S5.

Finally, we investigate the influence of meteorology on the 59% decrease in LDS burned area (Figure S9b-c). If meteorology played a major role, we would expect wetter and cooler conditions, or decreases in VPD and FWI over the 2003-2018 timeframe. In fact, we see the opposite – a 6% increase in VPD and 3% increase in FWI, although these trends are not statistically significant (Figure S9b-c). When detrended, however, VPD and FWI are moderately to strongly correlated with burned area, with the correlation $r = 0.57$ for VPD and $r = 0.79$ for FWI ($p < 0.05$). Thus, meteorology appears to drive the interannual variability but not the

decrease in LDS burned area over this time period that caused the fire season to shift earlier.

In summary, our approach using temporal shifts and distance to nearest fire strengthens the conclusion of previous studies that EDS prescribed burning, particularly in Arnhem Land, has shifted the fire season earlier and lowered LDS burned area and emissions.

3.4 Drivers of temporal shifts

In north India and the two case study regions — southwest Russia and north Australia — humans play an integral part in shaping the landscape by using prescribed burns, either to clear fields in an agricultural context or as a tool to prevent larger, more destructive fires in savannas. Although we do not find large changes in meteorological variability in line with the 39-day temporal shifts in the fire season, climate shocks, such as droughts and heatwaves, or concerns about rising greenhouse gas emissions may spur human actions that affect the use of fire, either through fire management or changes in government policy and agricultural practices. For example, in response to groundwater depletion and drought, state governments in north India delayed rice sowing closer to the monsoon onset, whereas in Russia, the federal government enacted wheat export bans and restrictions to protect domestic supply. In north Australia, Indigenous fire managers use prescribed burns to limit greenhouse gas emissions from LDS fires. Our probe of the potential human and climatic drivers is not exhaustive, and further study, such as through household surveys, is needed to systematically detail and confirm the mechanisms for the temporal shifts in each region described here, especially in southwest Russia.

Through the lens of the two case study regions, we briefly discuss five other ROIs, grouped by the two broad land cover types: croplands and savannas, grasslands, and shrublands. For croplands, the southwest Russia case study and studies on north India (Liu *et al* 2020a, Jethva *et al* 2019, Balwinder-Singh *et al* 2019) suggest that water stress, as well as increasing mechanization, modernization, and productivity, in agricultural systems are likely causes of changes in the timing of peak burning. In both south Russia and Thailand, the primary fire season coincides with the post-harvest period for spring wheat and rice, respectively (Hall *et al* 2016, Vadrevu *et al* 2015). GRACE observations of freshwater availability show an increase in south Russia of +0.52 cm yr^{-1} from 2003-2016, coinciding with earlier peak burning. Thailand, on the other hand, reveals a decline in freshwater availability of -0.53 cm yr^{-1} — that is, drought and/or groundwater depletion — coinciding with a delay in the fire season. For savannas, grasslands, and shrublands, the north Australia case study suggests that proactive fire management practices are key to limiting the fires with fast spread rates and high fuel consumption that occur later in the season. In contrast, poor fire management, in combination with drought, may drive fire seasons later. Fire is mainly used pasture management for grazing cattle in central Madagascar, whereas deforestation is common in Brazil, and careless use of fire, both deliberate and accidental, has led to destructive “veld” fires in Zimbabwe (Aragão *et al* 2018, Kull 2012, Nyamadzawo *et al* 2013). In fact, for Zimbabwe, Nyzmadzawo *et al* (2013) recommends a shift from fire suppression to fire management, with early season prescribed burns to curb the fire activity later in the season. Globally, Lipsett-Moore *et al* (2018) find potential in EDS prescribed burning to both mitigate fire emissions and improve livelihoods — aside from Australia — in 29 countries in Africa, 6 countries in South America, and Papua New Guinea.

4. Conclusion

In conclusion, we use 16 years of daily satellite-derived burned area to quantify the temporal shifts in the primary fire season at global scale. While earlier studies have diagnosed trends in annual fire activity (Andela *et al* 2017, Andela and van der Werf 2014, Giglio *et al* 2010), this is, to our knowledge, the first global study of trends in the timing of peak fire activity. We focus on regions where fires consistently recur year after year, and in particular, we select southwest Russia and north Australia as two case study regions, where the fire season has shifted by a total of nearly 40 days. No matter the setting, either croplands in southwest Russia or savannas in north Australia, we find human action to be likely the common denominator of these temporal shifts, although meteorological variability and climate change may drive these actions. Pinpointing regions where such shifts in the fire season occur is critical for contextualizing broader changes in agricultural systems, fire management practices, and government policies and for understanding the consequences of these changes. In India, government efforts to conserve water in spring have delayed the onset of rice residue burning during the post-monsoon season and inadvertently led to degraded air quality. In southwest Russia, human innovations and investment in agricultural technology and management have limited the need for fire to clear wheat residue. Meanwhile in north Australia, widespread adoption of indigenous fire management with increased prescribed burning have curbed the frequency of large fires over a broad region and potentially limited greenhouse gas emissions.

Data Availability

All data used in this study are publicly available. MODIS burned area and active fire datasets are distributed by NASA Earthdata (https://earthdata.nasa.gov/) and accessible through Google Earth Engine (http://earthengine.google.com/). The ERA5 reanalysis dataset is provided by ECWMF (https://www.ecmwf.int/). GRACE data are provided by NASA/JPL, University of Texas/CSR, and GFZ-Potsdam and also available on Google Earth Engine.

Acknowledgements

This work was supported by a National Science Foundation Graduate Research Fellowship awarded to T.L. (DGE1745303). We are grateful to Katie McGaughey, Cameron Yates, Owen Price, Andrew Edwards, Clare Murphy, Nicholas Deutscher, Elise-Andree Guerette, and Jenny Fisher for their helpful comments and insights.

References

Alcamo J, Dronin N, Endejan M, Golubev G and Kirilenko A 2007 A new assessment of climate change impacts on food production shortfalls and water availability in Russia *Glob. Environ. Chang.* **17** 429–44 Online: https://doi.org/10.1016/j.gloenvcha.2006.12.006

Andela N, Morton D C, Giglio L, Chen Y, van der Werf G R, Kasibhatla P S, DeFries R S, Collatz G J, Hantson S, Kloster S, Bachelet D, Forrest M, Lasslop G, Li F, Mangeon S, Melton J R, Yue C and Randerson J T 2017 A human-driven decline in global burned area *Science.* **356** 1356–62 Online: https://doi.org/10.1126/science.aal4108

366 Andela N, Morton D C, Giglio L, Paugam R, Chen Y, Hantson S, van der Werf G R and
367 Randerson J T 2019 The Global Fire Atlas of individual fire size, duration, speed, and
368 direction *Earth Syst. Sci. Data* **11** 529–52 Online: https://doi.org/10.5194/essd-2018-89

369 Andela N and van der Werf G R 2014 Recent trends in African fires driven by cropland
370 expansion and El Niño to la Niña transition *Nat. Clim. Chang.* **4** 791–5 Online:
371 https://doi.org/10.1038/nclimate2313

372 Andersen A N, Cook G D, Corbett L K, Douglas M M, Eager R W, Russell-Smith J, Setterfield
373 S A, Williams R J and Woinarski J C Z 2005 Fire frequency and biodiversity conservation
374 in Australian tropical savannas: Implications from the Kapalga fire experiment *Austral*
375 *Ecol.* **30** 155–67 Online: https://doi.org/10.1111/j.1442-9993.2005.01441.x

376 Ansell J, Evans J, Rangers A, Rangers A S, Rangers D, Rangers J, Rangers M, Rangers N N,
377 Rangers W, Rangers Y and Rangers Y M 2020 Contemporary Aboriginal savanna burning
378 projects in Arnhem Land: a regional description and analysis of the fire management
379 aspirations of Traditional Owners *Int. J. Wildl. Fire* **29** 371–85 Online:
380 https://doi.org/10.1071/WF18152

381 Aragão L E O C, Anderson L O, Fonseca M G, Rosan T M, Vedovato L B, Wagner F H, Silva C
382 V J, Silva Junior C H L, Arai E, Aguiar A P, Barlow J, Berenguer E, Deeter M N,
383 Domingues L G, Gatti L, Gloor M, Malhi Y, Marengo J A, Miller J B, Phillips O L and
384 Saatchi S 2018 21st Century drought-related fires counteract the decline of Amazon
385 deforestation carbon emissions *Nat. Commun.* **9** 536 Online:
386 https://doi.org/10.1038/s41467-017-02771-y

387 Artés T, Oom D, de Rigo D, Durrant T H, Maianti P, Libertà G and San-Miguel-Ayanz J 2019 A
388 global wildfire dataset for the analysis of fire regimes and fire behaviour *Sci. data* **6** 296

389 Balwinder-Singh, McDonald A J, Srivastava A K and Gerard B 2019 Tradeoffs between
390 groundwater conservation and air pollution from agricultural fires in northwest India *Nat.*
391 *Sustain.* **2** 580–3 Online: https://doi.org/10.1038/s41893-019-0304-4

392 Bowman D M J S, Kolden C A, Abatzoglou J T, Johnston F H, van der Werf G R and Flannigan
393 M 2020 Vegetation fires in the Anthropocene *Nat. Rev. Earth Environ.* Online:
394 https://doi.org/10.1038/s43017-020-0085-3

395 Chen Y, Morton D C, Andela N, van der Werf G R, Giglio L and Randerson J T 2017 A pan-
396 tropical cascade of fire driven by El Niño/Southern Oscillation *Nat. Clim. Chang.* **7** 906–11
397 Online: http://dx.doi.org/10.1038/s41558-017-0014-8

398 Deppermann A, Balkovič J, Bundle S C, Di Fulvio F, Havlik P, Leclère D, Lesiv M, Prishchepov
399 A V. and Schepaschenko D 2018 Increasing crop production in Russia and Ukraine -
400 Regional and global impacts from intensification and recultivation *Environ. Res. Lett.* **13**
401 025008 Online: https://doi.org/10.1088/1748-9326/aaa4a4

402 Evans J and Russell-Smith J 2020 Delivering effective savanna fire management for defined
403 biodiversity conservation outcomes: an Arnhem Land case study *Int. J. Wildl. Fire* **29** 386–
404 400 Online: https://doi.org/10.1071/WF18126

405 Fernandes P M and Botelho H S 2003 A review of prescribed burning effectiveness in fire
406 hazard reduction *Int. J. Wildl. fire* **12** 117–28 Online: https://doi.org/10.1071/WF01045

Giglio L, Boschetti L, Roy D P, Humber M L and Justice C O 2018 The Collection 6 MODIS burned area mapping algorithm and product *Remote Sens. Environ.* **217** 72–85 Online: https://doi.org/10.1016/j.rse.2018.08.005

Giglio L, Randerson J T, van der Werf G R, Kasibhatla P S, Collatz G J, Morton D C and DeFries R S 2010 Assessing variability and long-term trends in burned area by merging multiple satellite fire products *Biogeosciences* **7** 1171–86 Online: https://doi.org/10.5194/bg-7-1171-2010

Giglio L, Schroeder W and Justice C O 2016 The collection 6 MODIS active fire detection algorithm and fire products *Remote Sens. Environ.* **178** 31–41 Online: https://doi.org/10.1016/j.rse.2016.02.054

Götz L, Djuric I and Nivievskyi O 2016 Regional Price Effects of Extreme Weather Events and Wheat Export Controls in Russia and Ukraine *J. Agric. Econ.* **67** 741–63 Online: https://doi.org/10.1111/1477-9552.12167

Hall J V., Loboda T V., Giglio L and McCarty G W 2016 A MODIS-based burned area assessment for Russian croplands: Mapping requirements and challenges *Remote Sens. Environ.* **184** 506–21 Online: https://doi.org/10.1016/j.rse.2016.07.022

ICCI 2020 Krasnodar Krai Field Day: «Different Methods for the Use of Agricultural Residue other than Burning» Online: http://iccinet.org/wp-content/uploads/2012/03/Krasnodar-Field-Day-ENG-report-20141.pdf.

Jethva H, Torres O, Field R D, Lyapustin A, Gautam R and Kayetha V 2019 Connecting Crop Productivity, Residue Fires, and Air Quality over Northern India *Sci. Rep.* **9** 16594 Online: https://doi.org/10.1038/s41598-019-52799-x

Johnston F H, Henderson S B, Chen Y, Randerson J T, Marlier M E, DeFries R S, Kinney P, Bowman D M J S and Brauer M 2012 Estimated global mortality attributable to smoke from landscape fires *Environ. Health Perspect.* **120** 695–701 Online: https://doi.org/10.1289/ehp.1104422

Koplitz S N, Mickley L J, Marlier M E, Buonocore J J, Kim P S, Liu T, Sulprizio M P, DeFries R S, Jacob D J, Schwartz J, Pongsiri M and Myers S S 2016 Public health impacts of the severe haze in Equatorial Asia in September–October 2015: demonstration of a new framework for informing fire management strategies to reduce downwind smoke exposure *Environ. Res. Lett.* **11** 094023 Online: https://doi.org/10.1088/1748-9326/11/9/094023

Korontzi S, McCarty J, Loboda T, Kumar S and Justice C 2006 Global distribution of agricultural fires in croplands from 3 years of Moderate Resolution Imaging Spectroradiometer (MODIS) data *Global Biogeochem. Cycles* **20** GB2021

Kull C A 2012 Fire and people in tropical island grassland landscapes: Fiji and Madagascar *J. Pacific Stud.* **32** 121–9

Liefert O, Liefert W and Luebehusen E 2013 *Rising grain exports by the former Soviet Union region: Causes and outlook* Online: https://www.ers.usda.gov/webdocs/outlooks/39804/34899_whs13a01.pdf?v=44.4

Lipsett-Moore G J, Wolff N H and Game E T 2018 Emissions mitigation opportunities for savanna countries from early dry season fire management *Nat. Commun.* **9** 2247 Online:

https://doi.org/10.1038/s41467-018-04687-7

Liu J C, Mickley L J, Sulprizio M P, Dominici F, Yue X, Ebisu K, Anderson G B, Khan R F A, Bravo M A and Bell M L 2016 Particulate air pollution from wildfires in the Western US under climate change *Clim. Change* **138** 655–66 Online: http://dx.doi.org/10.1007/s10584-016-1762-6

Liu T, Marlier M E, Karambelas A, Jain M, Singh S, Singh M K, Gautam R and DeFries R S 2019 Missing emissions from post-monsoon agricultural fires in northwestern India: regional limitations of MODIS burned area and active fire products *Environ. Res. Commun.* **1** 011007 Online: https://doi.org/10.1088/2515-7620/ab056c

Liu T, Mickley L J, Gautam R, Singh M K, DeFries R S and Marlier M E 2020a Detection of delay in post-monsoon agricultural burning across Punjab, India: potential drivers and consequences for air quality *Environ. Res. Lett.* (in review) Online: https://doi.org/10.31223/osf.io/nh5w7

Liu T, Mickley L J, Singh S, Jain M, Defries R S and Marlier M E 2020b Crop residue burning practices across north India inferred from household survey data: bridging gaps in satellite observations *Atmos. Environ. X* (in press) Online: https://doi.org/10.1016/j.aeaoa.2020.100091

Nyamadzawo G, Gwenzi W, Kanda A, Kundhlande A and Masona C 2013 Understanding the causes, socio-economic and environmental impacts, and management of veld fires in tropical Zimbabwe *Fire Sci. Rev.* **2** 2 Online: https://doi.org/10.1186/2193-0414-2-2

Ojha N, Sharma A, Manish K, Girach I, Ansari T U, Sharma S K, Singh N, Pozzer A and Gunthe S S 2020 On the widespread enhancement in fine particulate matter across the Indo-Gangetic Plain towards winter *Sci. Rep.* **10** 5862 Online: https://doi.org/10.1038/s41598-020-62710-8

Pechony O and Shindell D T 2010 Driving forces of global wildfires over the past millennium and the forthcoming century *Proc. Natl. Acad. Sci. U. S. A.* **107** 19167–70 Online: https://doi.org/10.1073/pnas.1003669107

Petty A M and Bowman D M J S 2007 A Satellite Analysis of Contrasting Fire Patterns in Aboriginal- and Euro-Australian Lands in Tropical North Australia *Fire Ecol.* **3** 32–47

Petty A M, DeKoninck V and Orlove B 2015 Cleaning, Protecting, or Abating? Making Indigenous Fire Management "Work" in Northern Australia *J. Ethnobiol.* **35** 140–62 Online: https://doi.org/10.2993/0278-0771-35.1.140

Price O F 2015 Potential role of ignition management in reducing unplanned burning in Arnhem Land, Australia *Austral Ecol.* **40** 857–68 Online: https://doi.org/10.1111/aec.12264

Price O F, Russell-Smith J and Watt F 2012 The influence of prescribed fire on the extent of wildfire in savanna landscapes of western Arnhem Land, Australia *Int. J. Wildl. Fire* **21** 297–305 Online: https://doi.org/10.1071/WF10079

Rada N, Liefert W and Liefert O 2017 *Productivity Growth and the Revival of Russian Agriculture* Online: https://www.ers.usda.gov/webdocs/publications/83285/err-228.pdf?v=42844

Riley K L, Williams A P, Urbanski S P, Calkin D E, Short K C and O'Connor C D 2019 Will

Landscape Fire Increase in the Future? A Systems Approach to Climate, Fire, Fuel, and Human Drivers *Curr. Pollut. Reports* **5** 9–24 Online: https://doi.org/10.1007/s40726-019-0103-6

ROSSTAT 2020a *Socio-Economic Situation in Russia (In Russian: Социально-экономическое положение России)* Online: https://gks.ru/ (in Russian)

ROSSTAT 2020b Unified Interdepartmental Statistical Information System (UniSIS) [In Russian: Единая межведомственная информационно-статистическая система (ЕМИСС)] Online: https://fedstat.ru/ (in Russian)

Russell-Smith J, Edwards A C, Sangha K K, Yates C P and Gardener M R 2019 Challenges for prescribed fire management in Australia's fire-prone rangelands-the example of the Northern Territory *Int. J. Wildl. Fire* **29** 339–53 Online: https://doi.org/10.1071/WF18127

Schierhorn F, Faramarzi M, Prishchepov A V, Koch F J and Müller D 2014 Quantifying yield gaps in wheat production in Russia *Environ. Res. Lett.* **9** 084017 Online: https://doi.org/10.1088/1748-9326/9/8/084017

Shyamsundar P, Springer N P, Tallis H, Polasky S, Jat M L, Sidhu H S, Krishnapriya P P, Skiba N, Ginn W, Ahuja V, Cummins J, Datta I, Dholakia H H, Dixon J, Gerard B, Gupta R, Hellmann J, Jadhav A, Jat H S, Keil A, Ladha J K, Lopez-Ridaura S, Nandrajog S P, Paul S, Ritter A, Sharma P C, Singh R, Singh D and Somanathan R 2019 Fields on fire: Alternatives to crop residue burning in India *Science.* **365** 536–8 Online: https://doi.org/10.1126/science.aaw4085

Sidhu H S, Singh M, Yadvinder S, Blackwell J, Lohan S K, Humphreys E, Jat M L, Singh V and Singh S 2015 Development and evaluation of the Turbo Happy Seeder for sowing wheat into heavy rice residues in NW India *F. Crop. Res.* **184** 201–12 Online: https://doi.org/10.1016/j.fcr.2015.07.025

Sidorenko S, Trubilin E, Kolesnikova E and Hasegawa H 2017 Current Situation, Issues and Trends of Mechanization for Grain Harvesting in the Russian Federation *Agric. Mech. Asia, Africa, Lat. Am.* **48** 31–5

Singh K 2009 Act to Save Groundwater in Punjab: Its Impact on Water Table, Electricity Subsidy and Environment *Agric. Econ. Res. Rev.* **22** 365–386

de Sousa A 2019 The Pessimist's Guide to 2019: Fires, Floods, and Famine *Bloom. News* Online: https://www.bloomberg.com/graphics/pessimists-guide-to-2019/

Sulla-Menashe D, Gray J M, Abercrombie S P and Friedl M A 2019 Hierarchical mapping of annual global land cover 2001 to present: The MODIS Collection 6 Land Cover product *Remote Sens. Environ.* **222** 183–94 Online: https://doi.org/10.1016/j.rse.2018.12.013

Trauernicht C, Brook B W, Murphy B P, Williamson G J and Bowman D M J S 2015 Local and global pyrogeographic evidence that indigenous fire management creates pyrodiversity *Ecol. Evol.* **5** 1908–18 Online: https://doi.org/10.1002/ece3.1494

Tripathi A, Mishra A K and Verma G 2016 Impact of Preservation of Subsoil Water Act on Groundwater Depletion: The Case of Punjab, India *Environ. Manage.* **58** 48–59

USDA 2020 Crop Explorer - Commodity Intelligence Reports - Russian Federation Online: https://ipad.fas.usda.gov/cropexplorer/pecad_stories.aspx?regionid=rs&ftype=topstories

530 Vadrevu K P, Ellicott E, Badarinath K V S and Vermote E 2011 MODIS derived fire
531 characteristics and aerosol optical depth variations during the agricultural residue burning
532 season, north India *Environ. Pollut.* **159** 1560–9 Online:
533 https://doi.org/10.1016/j.envpol.2011.03.001

534 Vadrevu K P, Lasko K, Giglio L and Justice C 2015 Vegetation fires, absorbing aerosols and
535 smoke plume characteristics in diverse biomass burning regions of Asia *Environ. Res. Lett.*
536 **10**

537 Wegren S 2011 Food security and Russia's 2010 drought *Eurasian Geogr. Econ.* **52** 140–56
538 Online: https://doi.org/10.2747/1539-7216.52.1.140

539 Whitehead P J, Bowman D M J S, Preece N, Fraser F and Cooke P 2003 Customary use of fire
540 by indigenous peoples in northern Australia: Its contemporary role in savanna management
541 *Int. J. Wildl. Fire* **12** 415–25 Online: https://doi.org/10.1071/wf03027

542 Yibarbuk D, Whitehead P J, Russell-Smith J, Jackson D, Godjuwa C, Fisher A, Cooke P,
543 Choquenot D and Bowman D M J S 2001 Fire ecology and Aboriginal land management in
544 central Arnhem Land, northern australia: A tradition of ecosystem management *J. Biogeogr.*
545 **28** 325–43 Online: https://doi.org/10.1046/j.1365-2699.2001.00555.x

546 Zhang F, Wang J, Ichoku C, Hyer E J, Yang Z, Ge C, Su S, Zhang X, Kondragunta S, Kaiser J
547 W, Wiedinmyer C and da Silva A 2014a Sensitivity of mesoscale modeling of smoke direct
548 radiative effect to the emission inventory: A case study in northern sub-Saharan African
549 region *Environ. Res. Lett.* **9** 075002

550 Zhang X, Kondragunta S and Roy D P 2014b Interannual variation in biomass burning and fire
551 seasonality derived from geostationary satellite data across the contiguous United States
552 from 1995 to 2011 *J. Geophys. Res. Biogeosciences* **119** 1147–62 Online:
553 https://doi.org/10.1002/2013JG002518

554

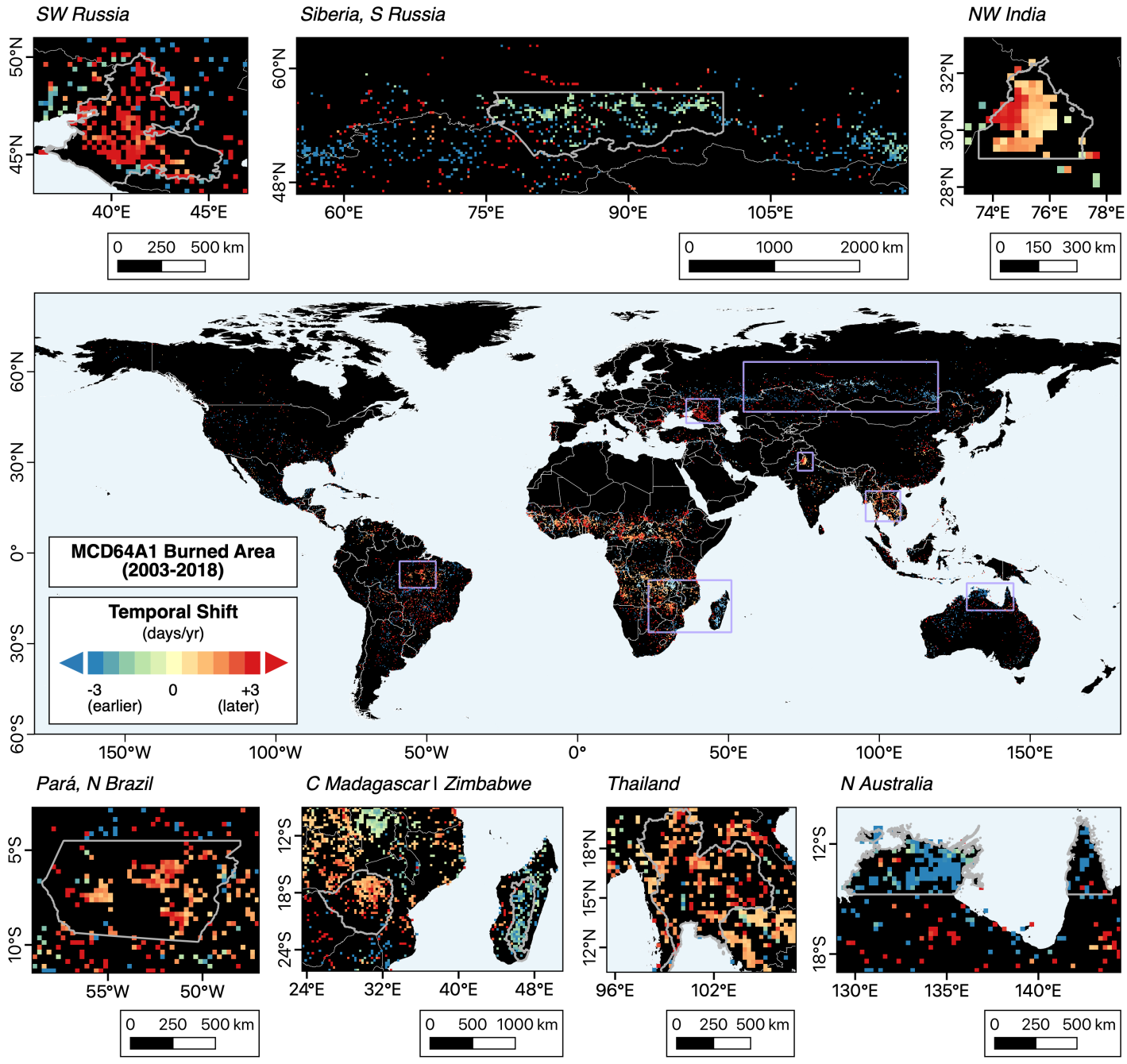

Figure 1. Temporal shifts in the midpoint of the primary fire season over a 16-year period from 2003-2018: The central panel shows regions of interest (outlined in purple), where coherent spatial signals in temporal shifts of MODIS MCD64A1 burned area (days yr^{-1}) are observed; smaller panels show zoomed-in maps with these regions outlined in gray. Only those grid cells with statistically significant trends ($p < 0.1$) are colored. Warm colors indicate fires occurring later over time, while cool colors represent fires occurring earlier over time.

563 **Table 1.** Regions of interest with coherent spatial signals of temporal shifts at the midpoint of
564 the primary fire season from 2003-2018. All trends are statistically significant at $p < 0.1$.

Code	Region	Provinces / States	Fire Season [start to end, Julian days]	Temporal Shift [days yr^{-1}; total 16-yr shift]
		1. Agricultural fires		
1a	NW India	Punjab, Haryana, Rajasthan [north of 29°N, east of 73.5°E]	250 to 340	+1.24 (20 days)
1b*	SW Russia	Krasnodar, Adygea, Rostov, Stavropol	140 to 330	+2.41 (39 days)
1c	S Russia	Omsk, Novosibirsk, Altai, Kemerovo, Khakassia, Krasnoyarsk, Tomsk, Irkutsk [south of 57.5°N]	70 to 150	-1.36 (22 days)
1d	Thailand	*all*	300 to 130	+0.64 (10 days)
		2. Savanna, grassland, and shrubland fires		
2a*	N Australia	Northern Territory, Queensland [north of 14.75°S]	90 to 365	-2.41 (39 days)
2b	C Madagascar	Anosy, Ihorombe, Haute Matsiatra, Amoron'i Mania, Vakinankaratra, Itasy, Bongolava, Analamanga, Betsiboka	100 to 365	-1.99 (32 days)
2c	Zimbabwe	*all*	110 to 350	+0.81 (13 days)
2d	N Brazil	Pará [south of 5.5°S]	190 to 300	+0.61 (10 days)

565 * Case study regions; N = North, S = South, W = West, E = East, C = Central

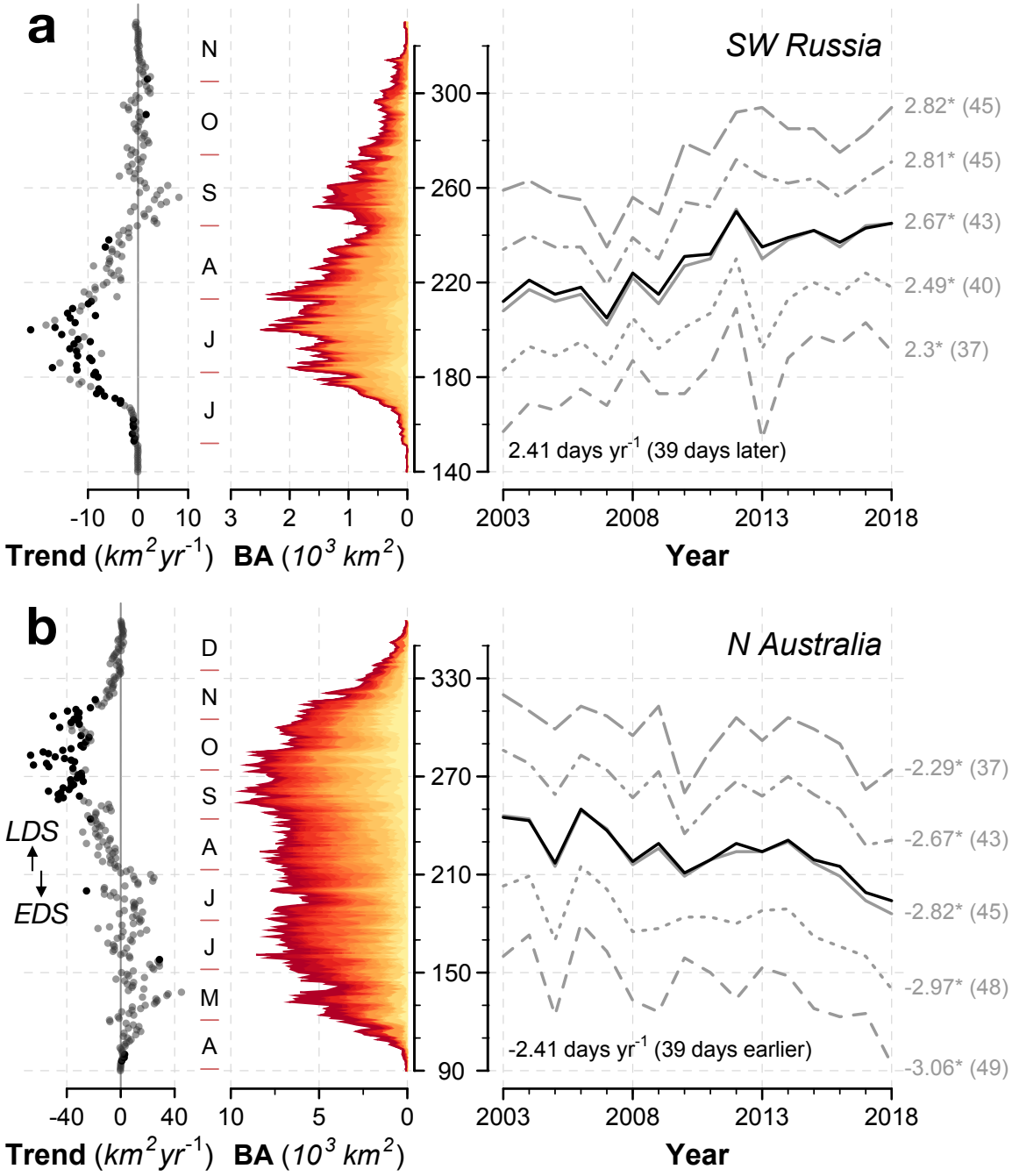

Figure 2. Regional temporal shifts in fire activity from 2003-2018 for two case study regions: Temporal shifts in MCD64A1 burned area for (**a**) southwest Russia and (**b**) north Australia and. *Left panels*: Trend in burned area by Julian day. Solid dots denote statistically significant trends at $p < 0.05$. *Middle panels*: Stacked burned area by day from 2003-2018. Redder colors denote later years. *Right panels*: Estimated breakpoints (e.g. start, end, midpoint) in primary fire season. Inset shows the temporal shift at the midpoint of the fire season using the weighted sums method (black line) and the total 16-year shift. Inset right shows the temporal shift for each breakpoint using the partial sums method (gray lines), and asterisks denote statistical significance at $p < 0.05$.

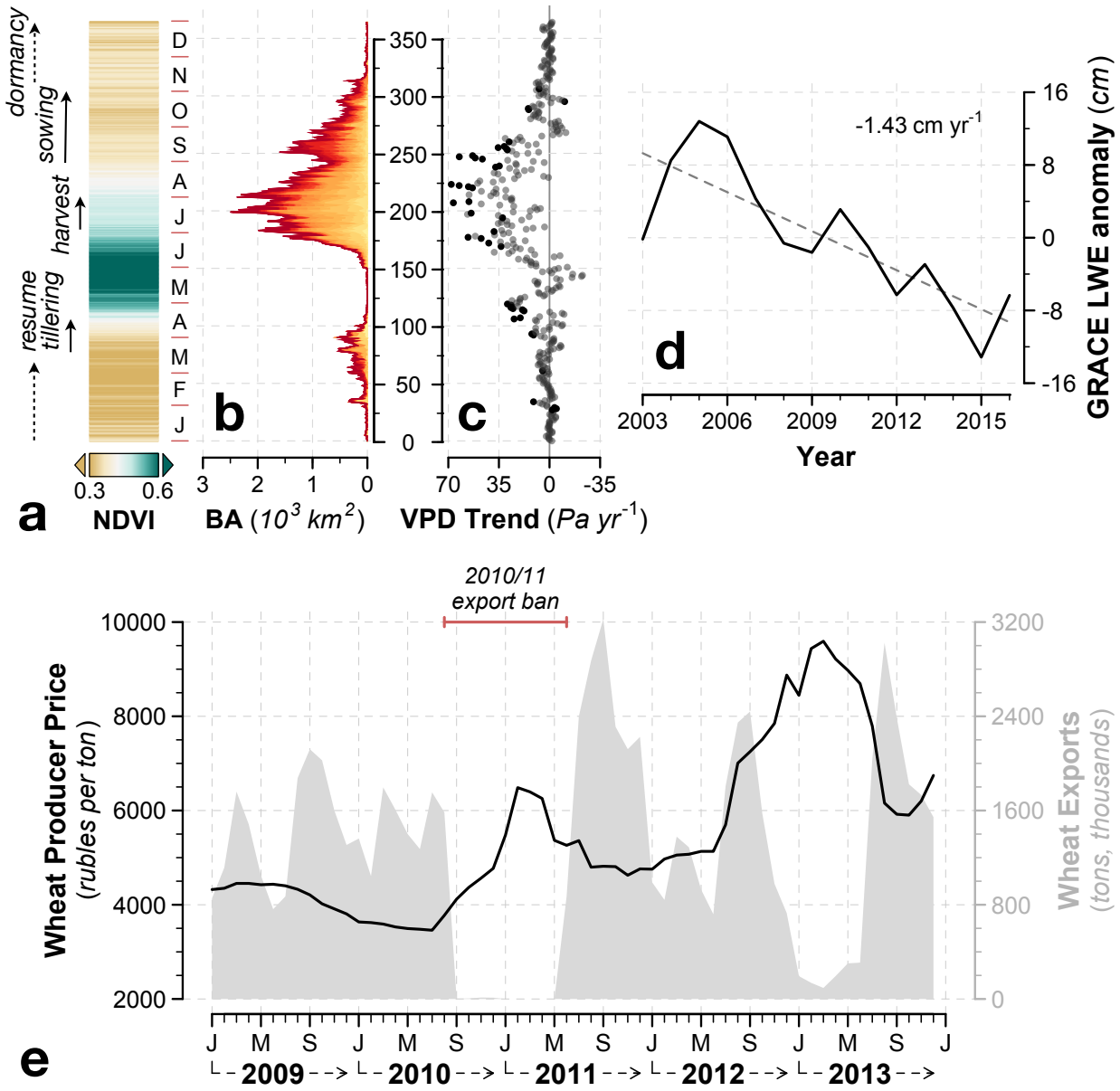

Figure 3. Winter wheat phenology, fire activity, and drought in southwest Russia: (**a**) Average 2003-2018 winter wheat phenology from MODIS-derived NDVI, with crop stages from the U.S. Department of Agriculture (https://ipad.fas.usda.gov/rssiws/al/crop_calendar/rs.aspx). (**b**) Aggregate burned area by day of year (same as Figure 2a but expanded to include the entire year). (**c**) Linear trend in ERA5 vapor pressure deficit (VPD) by day of year. Black dots denote statistical significance at $p < 0.05$. (**d**) Linear trend in annual GRACE freshwater storage availability, or the anomaly in equivalent liquid water thickness (LWE), from 2003-2016. **Wheat producer prices and export statistics in Russia from 2009-2013**: (**e**) Wheat producer price (black line) and export quantity (gray shading) (ROSSTAT 2020). The duration of the 2010/11 export ban is denoted as the red horizontal bar.

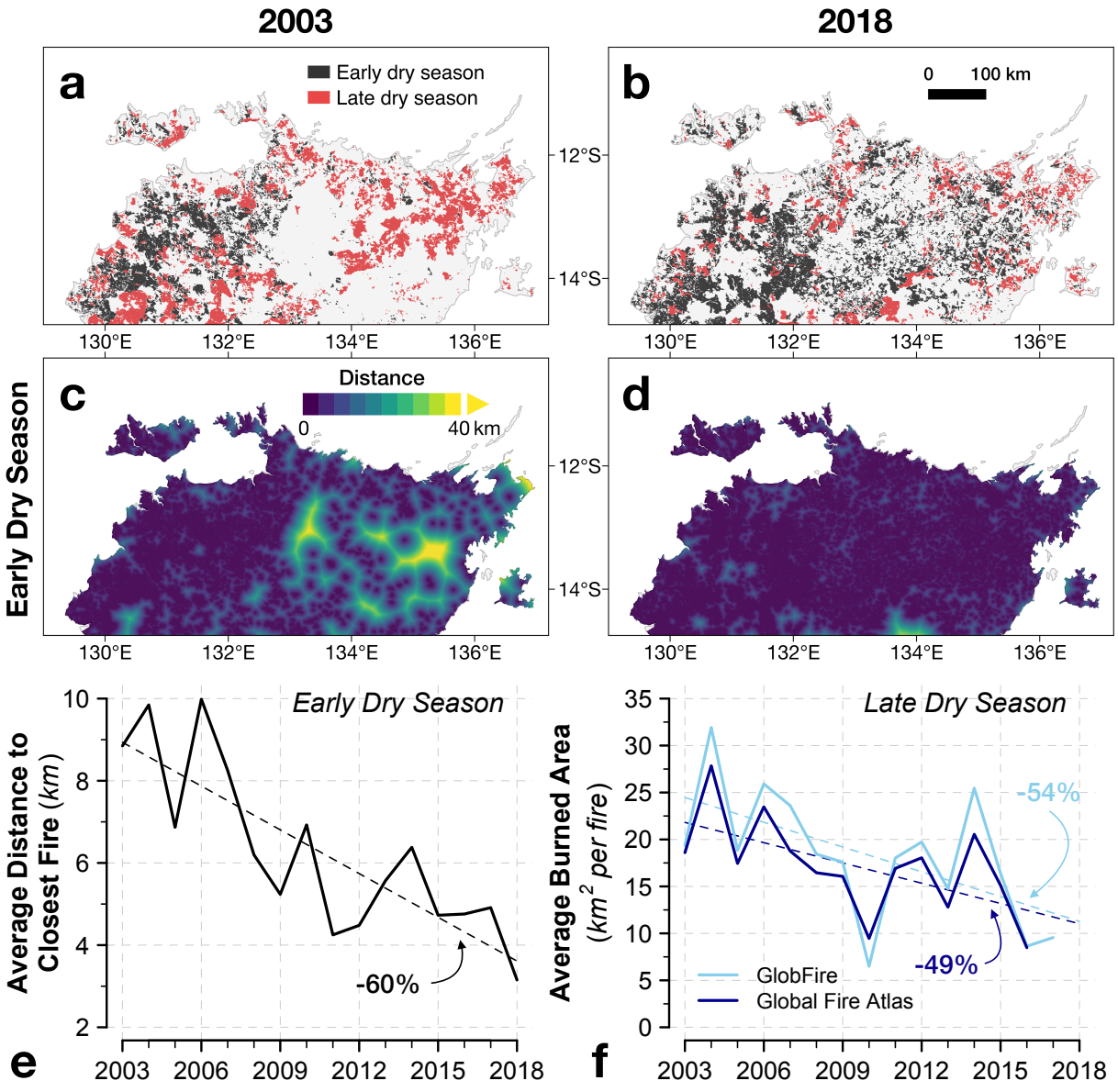

Figure 4. Trends in early and late dry season fires in north Australia from 2003-2018: Spatial comparison of MCD64A1 burned area during the early dry season (EDS, black shading) and late dry season (LDS, red shading) in the Top End of the Northern Territory in (**a**) 2003 and (**b**) 2018. Smaller islands without observed fire activity are excluded. Spatial distribution of the per-pixel distance in km to the closest burned area during the EDS in (**c**) 2003 and (**d**) 2018. The more uniform blue shading in 2018 indicates smaller distances between fires. (**e**) Annual trend in the distance to closest fire during the EDS from 2003 to 2018, averaged over all pixels in the Top End. This calculation excludes those pixels in which burning took place, i.e. areas with a distance of 0 km to the closest fire. Maximum distance is capped at 100 km. (**f**) Average burned area per fire (in km^2) during the LDS based on the GlobFire (2003-2017) and Global Fire Atlas (2003-2016) datasets (Artés *et al* 2019, Andela *et al* 2019). The linear trends shown in (**e**) and (**f**) are statistically significant at $p < 0.05$.